


## Deconfinement phase transition of thermal QED<sub>3</sub>

Yong-hui Xia,<sup>1</sup> Hong-tao Feng,<sup>2,\*</sup> and Hong-shi Zong<sup>1,†</sup>

<sup>1</sup>*Department of Physics, Nanjing University, Nanjing 210093, China*

<sup>2</sup>*School of Physics, Southeast University, Nanjing 211189, China*

 (Received 25 December 2017; revised manuscript received 20 August 2018; published 22 October 2018)

Since the dual fermion condensate be used to describe the center symmetry  $Z$ , we extend it to thermal QED<sub>3</sub> and study the deconfinement phase transition by the truncated Dyson-Schwinger equation for the massive fermion propagator at finite temperature. We show that, for a massive fermion, the system first appears as a deconfinement phase transition with the increase of temperature and then the chiral symmetry is restored and the corresponding temperature of the deconfinement phase transition increases with the enlargement of the fermion mass. It should be pointed out here that the results obtained in this paper are not model independent but are heavily dependent on the truncated Dyson-Schwinger equation we have chosen.

DOI: [10.1103/PhysRevD.98.074019](https://doi.org/10.1103/PhysRevD.98.074019)

### I. INTRODUCTION

Dynamical chiral symmetry breaking (DCSB) and confinement are two basic features of quantum chromodynamics (QCD). Due to the non-Abelian nature of QCD, and despite the effort made to study DCSB and confinement, it is still impossible to understand the physical mechanism of the above two basic characteristics of QCD from the first principle of QCD. In this case, it is very meaningful to try to study a relatively simple QCD-like system with physical properties of DCSB and confinement [1]. Fortunately, there is such a physical system in nature, the so-called three-dimensional quantum electrodynamic system (QED<sub>3</sub>). As a physical system with Abelian properties, it exhibits some nonperturbative features similar to QCD, such as DCSB and confinement. Moreover, it is superrenormalizable, so it does not suffer from the ultraviolet divergence that is present in QED<sub>4</sub>. Therefore, it can serve as a toy model of QCD. Besides, this model has been applied to some problems of condensed matter physics. In particular, QED<sub>3</sub> can be regarded as an effective model for high- $T_c$  superconductivity and the fractional quantum Hall effect [2–5] and also be widely used to explain the properties of strongly correlated systems [6–8].

As mentioned above, at zero temperature, QED<sub>3</sub> demonstrates the characteristics of DCSB [9] and confinement [10]. However, as the temperature rises, the chiral symmetry is restored and the deconfinement phase transition happens. The order parameter of the chiral phase transition is well defined via the trace of the fermion propagator in the chiral limit,

$$\langle \bar{\psi}\psi \rangle = \text{Tr}[S(x \equiv 0)] = \int \frac{d^3p}{(2\pi)^3} \frac{4B(p^2)}{A^2(p^2)p^2 + B^2(p^2)}, \quad (1)$$

where  $A(p^2)$ ,  $B(p^2)$  are related to the inverse fermion propagator  $S^{-1}(p) = i\gamma \cdot pA(p^2) + B(p^2)$ . It should be pointed out here that the above equation cannot be directly extended to the case beyond the chiral limit because Eq. (1) is ultraviolet (UV) divergence beyond the chiral limit and this divergence cannot be eliminated by a standard field-based renormalization process. For this reason, one has to use some regularization schemes to make the fermion condensate UV limited. At present, two regularization schemes are commonly used to eliminate ultraviolet divergence. One is to use the method of ultraviolet cutoff; see Refs. [11–13]. The other is to introduce offsets to eliminate UV divergence; see Refs. [14–17]. However, as pointed out in Ref. [15], the regularization by UV cutoff has a significant weakness—the obtained results depend on the UV cutoff. Therefore, in this paper, we will adopt a scheme to introduce offsets to eliminate the UV divergence of the fermion condensate. Specifically, the contribution of the “subtracted condensate” term introduced by the free fermion propagator is subtracted from the fermion condensate term, which can be expressed as

$$\langle \bar{\psi}\psi \rangle_m = 4 \int \frac{d^3p}{(2\pi)^3} \left[ \frac{B(p^2)}{A^2(p^2)p^2 + B^2(p^2)} - \frac{m}{p^2 + m^2} \right]. \quad (2)$$

The regularization scheme used above has two advantages:

(i) It is easy to find that when we introduce the “subtracted condensate” term, the right-hand side of Eq. (1) is UV

\*fenght@seu.edu.cn  
†zonghs@nju.edu.cn

finite. More interesting is that when “ $m$ ” approaches zero, Eq. (1) returns to the fermion condensate at the chiral limit. (ii) It is well known that only nonperturbative interactions can cause a phase transition in the system under study, while the vacuum condensate is a physical quantity that reflects the nonperturbative nature of the system. Therefore, properly reducing the influence of the perturbative interaction on the vacuum condensate is a requirement of the strong interaction theory itself.

To locate the temperature of the phase transition, the location of the peak of chiral susceptibility,

$$\chi^c = \frac{d\langle\bar{\psi}\psi\rangle_m}{dm}, \quad (3)$$

is considered as the phase transition temperature. Based on the Dyson-Schwinger equation (DSE) [18–23], one can investigate DCSB though the fermion propagator at zero and finite temperature. Now a problem arises naturally—the “subtracted condensate” term introduces a  $m$ -dependent term. Does this  $m$ -dependent term cause a change in the peak position of the regularized chiral susceptibility? We will discuss this below. The chiral susceptibility of the “subtracted condensate” is shown as follows:

$$\begin{aligned} \frac{\partial\langle\bar{\psi}\psi\rangle_s}{\partial m} &= \frac{\partial}{\partial m} \int^\Lambda \frac{d^3 p}{(2\pi)^3} \frac{4m}{p^2 + m^2} \\ &= \frac{2}{\pi^2} \int^\Lambda \frac{p^2 - m^2}{(p^2 + m^2)^2} p^2 dp \\ &= \frac{2}{\pi^2} (\Lambda - m\pi). \end{aligned} \quad (4)$$

As can be seen from the above equation, the “subtracted condensate” term only contributes a linearly dependent mass term, which obviously does not affect the location of the peak of the regularized chiral susceptibility.

How to determine deconfinement is a not a fully understood problem. In QCD, because of the center symmetry spontaneous breaking, the Polyakov loop is considered as an order parameter to determine the deconfinement phase transition in the limit of the large current quark mass since the dual quark condensate transforms as the dressed Polyakov loop under the center symmetry  $Z(N)$  transformation. Therefore, the dual fermion condensate in QCD can be considered as an order parameter to study the deconfinement phase transition [24–26]. By analogy with QCD, the additive group of the integers,  $Z$  symmetry, is spontaneous broken in the deconfinement phase of  $\text{QED}_3$ , which is investigated in Ref. [27]. Since  $\text{QED}_3$  exhibits a typical nonperturbative feature which is similar to QCD, it is valuable to generalize the dual fermion condensate to this Abelian system to investigate the confinement and deconfinement phase transition with the increasing temperature.

## II. DUAL FERMION CONDENSATE AND SYMMETRY $Z$

As is known to all, confinement is an open question in QCD. In the large quark mass limit, deconfinement is considered the result of center symmetry  $Z(N)$  breaking. However, in the case of the finite quark mass, the center symmetry is explicitly broken [28]. In Ref. [29], the authors introduce the imaginary chemical potential into the Lagrangian of QCD and find the relation between confinement and the remnant center symmetry  $Z(N)$  with finite quark mass. It should be noted that if the fermion mass is not infinite, there is explicit  $Z(N)$  breaking by the finite mass ( $m \neq \infty$ ) of the fermions, just as when the fermion mass is nonzero, there is finite explicit chiral symmetry breaking. This will definitely affect the chiral phase transition. The authors in Ref. [26] link the dressed Polyakov loop to the dual quark condensate because they both transform the same under the center symmetry  $Z(N)$ , and they find that the dual quark condensate can be used as an order parameter to describe the confinement-deconfinement phase transition.

Moreover, the authors express the relation between  $Z$  symmetry and confinement in  $\text{QED}_3$  [27]. In the confined phase, the effective potential  $V$  with the one-loop approximation is given by

$$\begin{aligned} V &= -\frac{T^2}{\pi} \left[ \frac{m}{T} \text{Li}_2(e^{-m/T}, eA_0/T + \pi) \right. \\ &\quad \left. + \text{Li}_3(e^{-m/T}, eA_0/T + \pi) \right], \end{aligned} \quad (5)$$

where  $m$  denotes the fermion mass. Here,  $A_0 = a(r)/\sqrt{T}$ ,  $\text{Li}_2(r, \theta) = \int_0^r dx \ln(1 - 2x \cos \theta + x^2)/2x$ , and  $\text{Li}_3(r, \theta) = \int_0^r dx \text{Li}_2(x, \theta)/x$ . The effective potential shows an obvious periodicity for  $eA_0 \rightarrow eA_0/T + 2\pi$ . However, in the deconfinement phase, we have  $\langle A_0 \rangle = 2\pi nT/e$ . Then, the effective potential  $V$  becomes constant, and the  $Z$  symmetry is spontaneously broken. In a semiclassical view, the nonzero expectation value of the zero component of the gauge potential can be regarded as an imaginary chemical potential for the fermions. Therefore, in an interesting attempt, we extend the dual fermion condensate from QCD to  $\text{QED}_3$  and study the deconfinement phase transition in the Abelian system.

From Ref. [24], the order parameter  $P_l(m)$  describing the confinement-deconfinement phase transition in QCD is obtained by the dual fermion condensate,

$$P_l(m) = - \int_0^{2\pi} \frac{d\phi}{2\pi} e^{-i\phi} \langle\bar{\psi}\psi\rangle_m(\phi), \quad (6)$$

where  $\langle\bar{\psi}\psi\rangle_m(\phi)$  is the ordinary fermion condensate using the  $U(1)$ -valued boundary conditions with the angle  $\phi$  in the temporal direction of the Euclidean space. In analogy

with QCD, we find the relation between the dressed Polyakov loop and the dual fermion condensate.

Following the inspiration of Refs. [24–26], we try to reveal the relation between the dual fermion condensate and the symmetry Z in QED<sub>3</sub>. In Euclidean space, the Lagrangian of QED<sub>3</sub> with the massive fermion reads

$$\mathcal{L} = \bar{\psi}(\not{\partial} + ie\mathbf{A} + m)\psi + \frac{1}{4}F_{\mu\nu}^2 + \frac{1}{2\xi}(\partial_\nu A_\nu)^2, \quad (7)$$

where the four-component spinors are employed.

According to the procedure of lattice regularization [26], the condensate with the U(1)-valued boundary condensate  $\langle \bar{\psi}\psi \rangle_m(\phi)$  can be expressed in powers of the Dirac operator,

$$\langle \bar{\psi}\psi \rangle_m(\phi) = \frac{1}{m} \sum_{k=0}^{\infty} \frac{(-1)^k}{m^k} \langle \text{Tr}[D_\phi^k] \rangle, \quad (8)$$

where  $D_\phi$  is the staggered lattice Dirac operator shown as follows,

$$D_{xy} = \sum_{j=1}^3 \frac{\eta_j}{2a} [U_j(x)\delta_{x+\hat{j},y} - \text{H.c.}] \quad (9)$$

with the staggered sign function  $\eta_j = (-1)^{x_1+\dots+x_{j-1}}$ . The lattice spacing  $a$  and  $U$  denote the gauge link variables. Inserting the Dirac operator Eq. (9) into Eq. (8), then, the dual fermion condensate can be written as follows,

$$\langle \bar{\psi}\psi \rangle_m(\phi) = \frac{1}{m} \sum_{l \in \mathcal{L}} \frac{s(l)e^{i\phi q(l)}}{(2am)^{|l|}} \langle \prod_{(x,j) \in l} U_j \rangle, \quad (10)$$

Where the set  $\mathcal{L}$  denotes all possible closed loops on the lattice,  $s(l)$  denotes the sign of a particular loop  $l$  obtained as product of the staggered sign factors,  $|l|$  denotes the length of the loop  $l$ . The winding number  $q(l) \in \mathbb{Z}$  is obtained by the loop  $l$  winding around the compact time direction and the factor  $\exp(i\phi q(l))$  denotes the loops winding forward around the compact time direction. We perform a Fourier transformation on Eq. (10), and the dual fermion condensate is given by

$$P_l(m) = -\frac{1}{m} \sum_{l \in \mathcal{L}(1)} \frac{s(l)}{(2am)^{|l|}} \langle \prod_{(x,j) \in l} U_j \rangle. \quad (11)$$

Here, we need to emphasize that the subtracted condensate is not the same as that which appears in Eqs. (8)–(11). In this paper, the subtracted condensate is adopted as a free fermion condensate at zero temperature and the Fourier factor  $e^{-i\phi}$  is a project operator to pick up the loop with winding number 1. Now, it is easy to find the relation between the dual fermion condensate and the symmetry Z. Under the group Z transformation, we have  $U_3(x, t_0) \rightarrow zU_3(x, t_0)$ , where  $z$  represents the elements of

the group Z. Then, the dual fermion condensate follows the same transformation:  $P_l(m) \rightarrow zP_l(m)$ . At low temperature, the symmetry Z is kept, and we have  $P_l(m) = zP_l(m)$ , and then  $P_l(m) = 0$ . With the temperature increasing, at the critical temperature  $T_c$ , the symmetry Z is broken, and we have  $P_l(m) \neq 0$ . Thus, the dual fermion condensate can be regarded as an order parameter of the deconfinement phase transition in thermal QED<sub>3</sub>. It should be noted that Eq. (8) is strictly valid when the (bare) fermion mass is large enough. Here, following the inspiration of Refs. [24–26], we perform an analytic continuation of Eq. (8) into the region of small fermion mass.

### III. DYSON-SCHWINGER EQUATION WITH $\phi$

To gain the dual fermion condensate and analyze the deconfinement, we adopt the DSEs for the fermion propagator,

$$S^{-1}(p) = i\gamma \cdot p + m + \int \frac{d^3k}{(2\pi)^3} \gamma_\mu S(k) \Gamma_\nu(p, k) D_{\mu\nu}(p-k), \quad (12)$$

where the unit  $e^2 = 1$  and the boson propagator  $D_{\mu\nu}(q)$  in the Landau gauge are given as

$$D_{\mu\nu}(q) = \frac{\delta_{\mu\nu} - q_\mu q_\nu / q^2}{q^2 + \Pi(q^2)}. \quad (13)$$

The self-consistent coupled DSEs, where the full fermion and boson propagators are involved, reveal the confinement behaviors of QED<sub>3</sub> at zero temperature and density [10,30]. It is very interesting to recall the corresponding perturbative results for the dressing of the photon propagator by the fermions: if the massless fermions are introduced,  $\Pi(q^2) \propto q$ , and the potential becomes Columbia at long distances where the fermion will not be confined; however, if the massive fermions are employed,  $\Pi(q^2)/q^2 \rightarrow \frac{4}{3\pi m}$  in the infrared region, and the confining property appears [10]. To extend the dual fermion condensate to the Abelian system, we try to analyze the case of massive fermions to give insight into the deconfinement of QED<sub>3</sub> with the increase of temperature.

At finite temperature T, the inverse fermion propagator is written as

$$S_\phi^{-1}(P) = i\gamma_0 \varpi_n(\phi) A_\phi(P^2) + i\vec{\gamma} \vec{p} C_\phi(P^2) + B_\phi(P^2), \quad (14)$$

where  $\varpi_n(\phi) = (2n+1)\pi T + \phi T$  and the boundary conditions for fermions requires  $\phi = 0$ , while  $\phi = \pi$  corresponds to bosons.

Now, let us review some studies on the effect of the wave function renormalization factor  $A$  and  $C$ . In the past, the lowest-order approximation, *i.e.*,  $A = C = 1$ , is often adopted to calculate the critical fermion flavor [31–33], and

the results show that, although the influence of  $A$ ,  $C$  can change the numerical results, the low-order approximation of DSE of the fermion propagator still contains qualitative nonperturbative properties of QED<sub>3</sub> at zero temperature. However, just as Ref. [33] suggested, one should treat renormalization factor  $A$  and  $C$  carefully at finite temperature. Indeed, it is important to obtain  $A$ ,  $C$  beyond the lowest-order approximation in the case of finite temperature, but the numerical calculation is complex and it is difficult to

obtain the stable numerical solutions. In this paper, the dual fermion condensate is extended to QED<sub>3</sub> to study the deconfinement phase transition. In order to obtain the results qualitatively, as the first step of attempt, the lowest-order approximation is still adopted to perform numerical calculation to study deconfinement phase transition.

Then, taking into account the finite temperature, the integral equation for the dynamically generated fermion self-energy function with  $\phi$  reduces to

$$B_\phi(P^2) = m + \sum_n \int \frac{d^2K}{(2\pi)^2} \frac{2TB_\phi(K^2)}{[\varpi_n(\phi)^2 + \mathcal{E}_\phi^2(K^2)][Q^2 + \Pi_0(Q^2)]} = m + \frac{1}{2} \int \frac{d^2K}{(2\pi)^2} \frac{B_\phi(K^2) \tanh \frac{\mathcal{E}_\phi(K^2) \pm i\phi T}{2T}}{\mathcal{E}_\phi(K^2)[Q^2 + \Pi_0(Q^2)]}, \quad (15)$$

where  $\mathcal{E}_\phi(K^2) = \sqrt{K^2 + B_\phi^2(K^2)}$ ,  $\tanh \frac{\mathcal{E}_\phi(K^2) \pm i\phi T}{2T} \equiv \tanh \frac{\mathcal{E}_\phi(K^2) + i\phi T}{2T} + \tanh \frac{\mathcal{E}_\phi(K^2) - i\phi T}{2T}$ , and the Matsubara frequency is summed analytically. The corresponding boson polarization is given by [31]

$$\Pi_0(Q^2) = \frac{T}{\pi} \int_0^1 dx \left\{ \ln \left( 4 \cosh^2 \frac{\sqrt{m^2 + x(1-x)Q^2}}{2T} \right) - \frac{m^2 \tanh \frac{\sqrt{m^2 + x(1-x)Q^2}}{2T}}{T \sqrt{m^2 + x(1-x)Q^2}} \right\}. \quad (16)$$

In principle, the boson polarization should depend on  $\phi$  as it depends on chemical potential in the finite chemical potential case [34]. However, we cannot find the stable numerical solution under the current truncation scheme of the DSE approach. At the moment, we can only ignore the dependence of  $\phi$  on the boson propagator to study the confinement in QED<sub>3</sub>, but this is definitely worth further discussion.

The regularized fermion condensate with  $\phi$  at finite temperature is obtained:

$$\begin{aligned} \langle \bar{\psi}\psi \rangle_m(\phi) &= 4T \sum_n \int \frac{d^2P}{(2\pi)^2} \frac{B_\phi(P^2)}{\varpi_n^2(\phi) + \mathcal{E}_\phi^2(P^2)} - \int \frac{d^3p}{(2\pi)^3} \frac{4m}{p^2 + m^2} \\ &= \int \frac{d^2P}{(2\pi)^2} \frac{B_\phi(P^2) \tanh \frac{\mathcal{E}_\phi(P^2) \pm i\phi T}{2T}}{\mathcal{E}_\phi(P^2)} - \int \frac{d^3p}{(2\pi)^3} \frac{4m}{p^2 + m^2}. \end{aligned} \quad (17)$$

Here, because the divergence term comes from the zero temperature, the subtracted term is chosen at zero temperature and  $\phi = 0$  in this paper. We need to emphasize here that we only subtract the trace of the free propagator at zero temperature rather than the free propagator at the finite temperature, because the latter introduces nontrivial temperature-dependent effects on the regularized quark condensate.

#### IV. FERMION CONDENSATE

Next, we numerically resolve Eq. (15) by application of iteration and plot the evolution of the fermion self-energy function with temperature and  $\phi$  value in Figs. 1–3. The dependence of fermion condensate on  $\phi$  with a range of temperature and fermion mass are shown in Figs. 4–6. From Figs. 1–3, it is easy to find that the fermion self-energy is obviously larger than the bare fermion mass at  $P^2 = 0$  with different  $\phi$ . With the increases of momenta, the  $B(P^2)$  approach the bare fermion mass. Thus, on one

hand, the regularized condensate, which obtained by subtracting the condensate of free fermion at zero temperature, is nonzero within the temperature range studied; on the other hand, the  $\phi$  dependence condensate is always

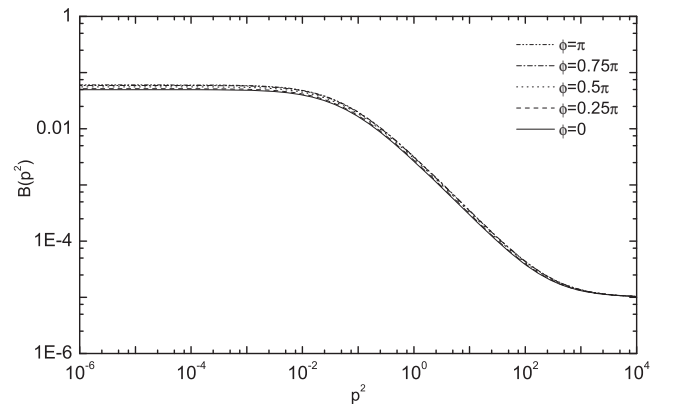


FIG. 1. The dependence of  $B(P^2)$  on  $P^2$  at  $T = 0.02$  with  $m = 10^{-5}$ .

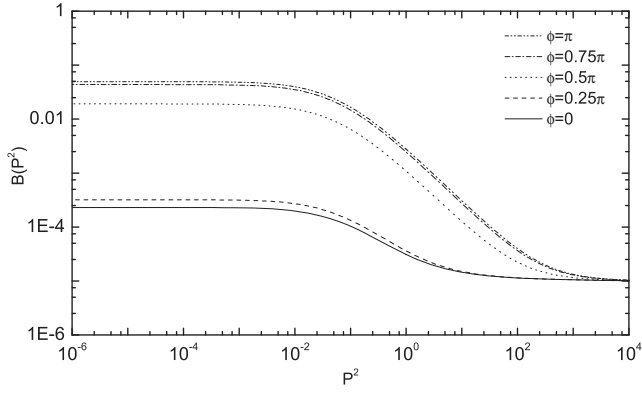


FIG. 2. The dependence of  $B(P^2)$  on  $P^2$  at  $T = 0.03$  with  $m = 10^{-5}$ .

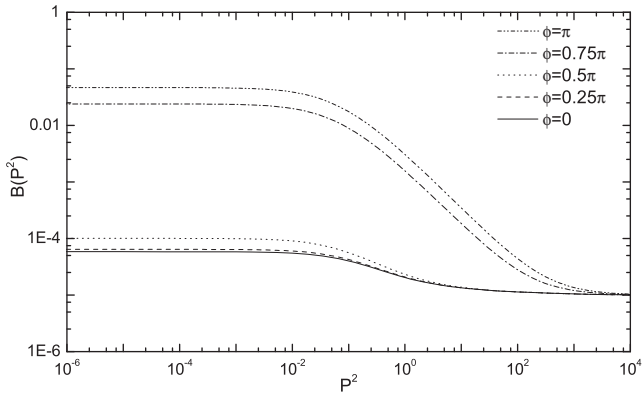


FIG. 3. The dependence of  $B(P^2)$  on  $P^2$  at  $T = 0.05$  with  $m = 10^{-5}$ .

depend on  $\phi$  and the dressed Polyakov loop would not be zero at high temperature. From Figs. 4–6, it is also easy to find that, whether the chiral limit or the nonchiral limit, the  $\phi$ -dependent condensate is almost flat when the temperature is low, which results in the Polyakov loop being small. With the increase of temperature, the curve shows an arch

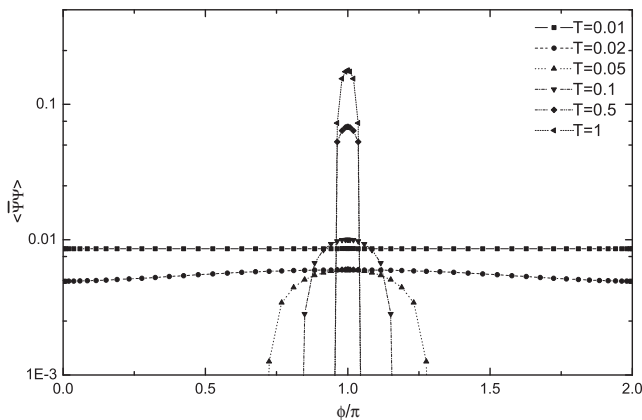


FIG. 4. The dependence of  $\langle \bar{\psi}\psi \rangle$  on  $\phi$  with a range of temperature in the chiral limit.

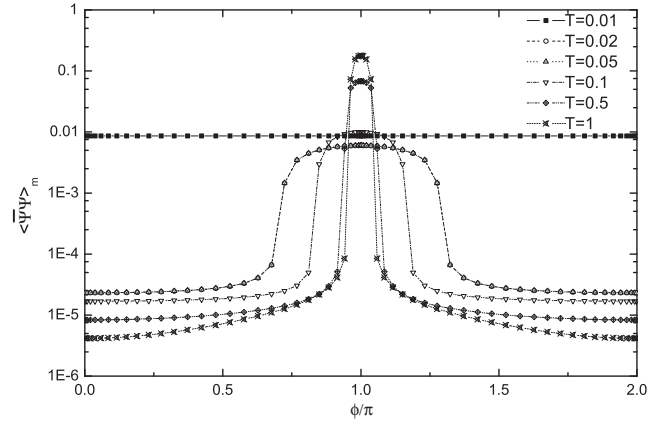


FIG. 5. The dependence of  $\langle \bar{\Psi}\Psi \rangle_m$  on  $\phi$  with a range of temperature at  $m = 10^{-5}$ .

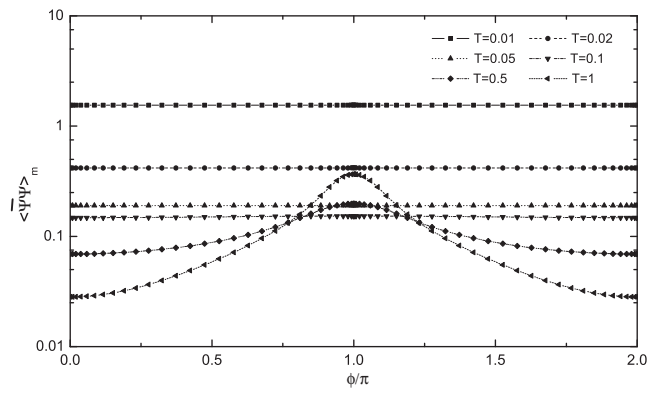


FIG. 6. The dependence of  $\langle \bar{\psi}\psi \rangle_m$  on  $\phi$  with a range of temperature at  $m = 0.1$ .

symmetry at the  $\phi = \pi$  axis. Moreover, we find that the width of the peak narrows with the increasing temperature.

The next step is to investigate the influence of temperature on the dual fermion condensate. Figure 7 shows the evolution of the fermion condensate and dual fermion

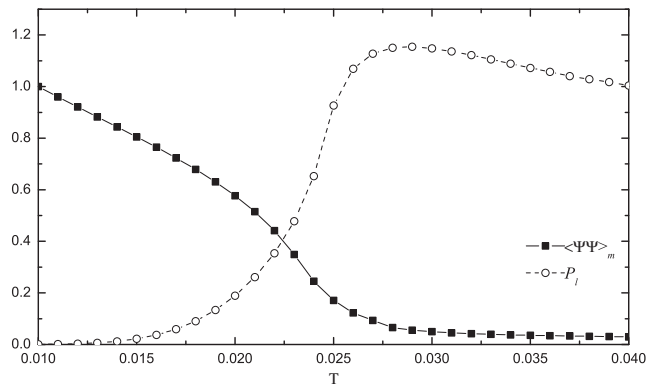


FIG. 7. The dependence of dual fermion condensate and fermion chiral condensate on temperature for  $m = 10^{-5}$ , where  $\langle \bar{\Psi}\Psi \rangle_m$  is normalized by its value at  $T = 0.01$  and  $P_l$  is normalized by its value at  $T = 0.04$ .



condensate with temperature. From Fig. 7, it is found that, at  $T \rightarrow 0$ , the dual fermion condensate has a small, in fact, zero value but increases with the rise of temperature. Meanwhile, the normalized fermion chiral condensate gradually decreases. It should be noted here that the fermion condensate is nonzero at high temperature, so the self-energy is larger than the bare fermion mass in the infrared region within the temperature range studied.

## V. PHASE TRANSITION AT FINITE TEMPERATURE

In order to give an insight into the critical point of the chiral and deconfinement phase transitions, we adopt chiral susceptibility which measures the response of the chiral condensate to an infinitesimal change of fermion mass,

$$\chi^c = \frac{d}{dm} \langle \bar{\psi}\psi \rangle_m, \quad (18)$$

as the probe for locating the temperature of the chiral phase transition and dual susceptibility which denote the differential coefficient of dual fermion condensate to temperature [24,25],

$$\chi^d(T) = \frac{dP_l}{dT}, \quad (19)$$

for deconfinement. After solving the truncated DSE (15) by means of the iteration method, we can obtain the evolution of the two susceptibilities with temperature. A plot of the chiral and dual susceptibilities with little fermion mass change with temperature around the critical point is shown in Fig. 8. For a fixed fermion mass, as the temperature rises, each of the two susceptibilities illustrates a smooth peak, which means crossover. Here, the transition temperature is

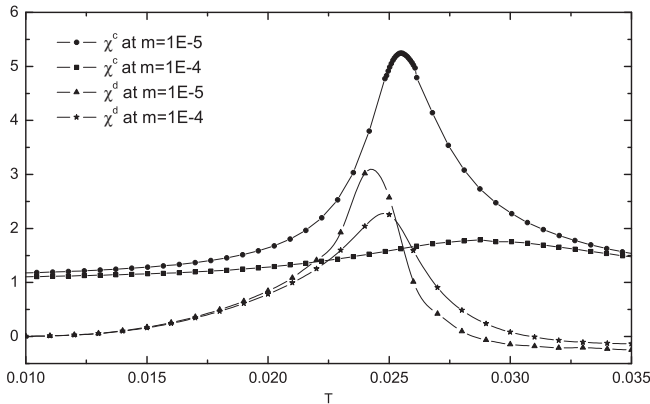


FIG. 8. The behaviors of chiral and dual susceptibilities around the critical temperature with the increasing temperature. Here, we need to make an annotation. In order to make  $\chi^c$  and  $\chi^d$  compare in one graph, we intentionally expand the  $\chi^d$  in the graph by 10 times than the corresponding actual calculated value.

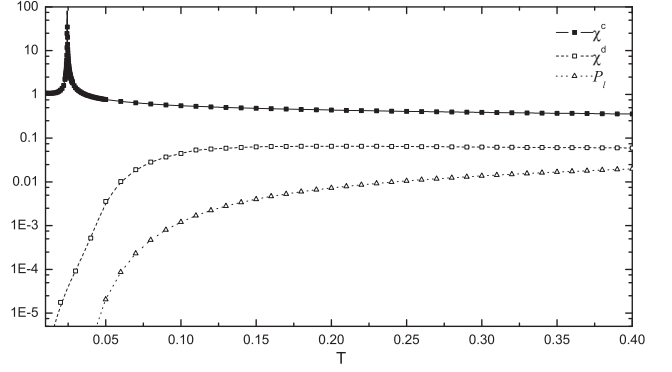


FIG. 9. The chiral susceptibility in the chiral limit and dual susceptibility and dual condensate with  $m = 0.1$  as a function of temperature. Here we need to make an annotation. In order to make the three curves clearly expressed in one graph, we intentionally expand the  $\chi^d$  and  $P_l$  in the graph by 100 times the corresponding actual calculated value.

located by peak of the curves. It is easy to find that the pseudocritical temperature of chiral transition is obviously larger than that of deconfinement transition temperature. This indicates that the deconfinement transition occurs earlier than chiral transition in the approximate framework used in our paper, which is different from QCD. In QCD, beyond the chiral limit, the lattice simulations [35,36] show that the pseudochiral transition and pseudodeconfinement transition occur at the same temperature. Moreover, with the increase of the fermion mass, the curve of chiral susceptibility trends to flat, which is what we expect. This is because the chiral symmetry is no longer a good symmetry in the case of the large fermions masses. Thus, one generally expects that at large fermions masses, the chiral phase transition is severely softened.

In order to compare with the change of the chiral and dual susceptibilities at finite temperature in the small fermion mass case in Fig. 8, we plot the variation of the chiral susceptibility with temperature in the chiral limit and the dual condensate and the dual susceptibility as a function of temperature in the case of the large fermion mass ( $m = 0.1$ ) in Fig. 9. In the chiral limit, from the Fig. 9, one can find that the chiral susceptibility diverges at  $T = 0.025$ . Therefore, the chiral phase transition is a second-order phase transition in the chiral limit. However, beyond the chiral limit, even if there is only a very small fermion mass, the chiral transition will become crossover (see Fig. 8). For the case of dual susceptibility with  $m = 0.1$ , Fig. 9 shows that the dual susceptibility has a smooth peak at  $T = 0.19$  and the transition is still a crossover.

## VI. CONCLUSIONS

The purpose of this paper is to generalize the dual fermion condensate to QED<sub>3</sub> and investigate the chiral phase transition and the deconfinement phase transition of thermal QED<sub>3</sub> through a continuum study of the

Dyson-Schwinger equation. To this end, we introduced a regularized fermion condensate that not only eliminates the UV divergence but also properly describes the nonperturbative characteristics of QED<sub>3</sub>. Based on this regularized fermion condensate, we systematically studied the evolution of the chiral and dual susceptibilities with temperature. It is found that, with the increase of temperature, the above two susceptibilities all show smooth peaks, which indicates that the chiral transition and the deconfinement transition of QED<sub>3</sub> at finite temperature are crossover (The transitions are crossover because of the presence of explicit breaking.). More interestingly, in the DSE truncation framework used in this paper, we found that in QED<sub>3</sub> with finite temperature, the deconfinement transition occurred earlier than the

corresponding chiral transition. Obviously, all the conclusions drawn in this paper are based on our model approximation and are heavily dependent on the model framework we use. Trying to pursue a good model approximation should be the direction of our future efforts.

## ACKNOWLEDGMENTS

We would like to thank Professor C. D. Roberts and Lei Chang for their helpful discussions. This work is supported in part by the National Natural Science Foundation of China (under Grants No. 11475085, No. 11535005, and No. 11690030) and by Nation Major State Basic Research and Development of China (2016YFE0129300).

- 
- [1] G. Z. Liu and G. Cheng, *Phys. Rev. D* **67**, 065010 (2003).
  - [2] W. Rantner and X. G. Wen, *Phys. Rev. Lett.* **86**, 3871 (2001).
  - [3] M. Franz and Z. Tesanovic, *Phys. Rev. Lett.* **87**, 257003 (2001); I. F. Herbut, *Phys. Rev. Lett.* **88**, 047006 (2002); *Phys. Rev. B* **66**, 094504 (2002); *Phys. Rev. Lett.* **94**, 237001 (2005).
  - [4] X. G. Wen and A. Zee, *Phys. Rev. Lett.* **69**, 1811 (1992).
  - [5] G. Z. Liu and G. Cheng, *Phys. Rev. B* **66**, 100505 (2002).
  - [6] J. Wang, P. L. Zhao, J. R. Wang, and G. Z. Liu, *Phys. Rev. B* **95**, 054507 (2017).
  - [7] J. R. Wang and G. Z. Liu, *Phys. Rev. B* **89**, 195404 (2014).
  - [8] J. R. Wang, G. Z. Liu, and C. J. Zhang, *Phys. Rev. D* **91**, 045006 (2015).
  - [9] T. Appelquist, D. Nash, and L. C. R. Wijewardhana, *Phys. Rev. Lett.* **60**, 2575 (1988).
  - [10] P. Maris, *Phys. Rev. D* **52**, 6087 (1995).
  - [11] T. Meissner, *Phys. Lett. B* **405**, 8 (1997).
  - [12] H. S. Zong and X. F. Lü, J. Z. Gu, C. H. Chang, and E. G. Zhao, *Phys. Rev. C* **60**, 055208 (1999).
  - [13] H. S. Zong and X. F. Lü, F. Wang, C. H. Chang, and E. G. Zhao, *Commun. Theor. Phys.* **34**, 563 (2000).
  - [14] M. He, Y. Jiang, W. M. Sun, and H. S. Zong, *Phys. Rev. D* **77**, 076008 (2008).
  - [15] H. S. Zong, J. L. Ping, H. T. Yang, and X. F. Lü, and F. Wang, *Phys. Rev. D* **67**, 074004 (2003).
  - [16] Y. Aoki, G. Endrődi, Z. Fodor, S. D. Katz, and K. K. Szabó, *Nature (London)* **443**, 675 (2006).
  - [17] Y. Aoki, Z. Fodor, S. D. Katz, and K. K. Szabó, *Phys. Lett. B* **643**, 46 (2006).
  - [18] C. S. Fischer, R. Alkofer, T. Dahm, and P. Maris, *Phys. Rev. D* **70**, 073007 (2004).
  - [19] H. T. Feng, D. K. He, W. M. Sun, and H. S. Zong, *Phys. Lett. B* **661**, 57 (2008).
  - [20] A. Ayala and A. Bashir, *Phys. Rev. D* **67**, 076005 (2003).
  - [21] H. T. Feng, *Mod. Phys. Lett. A* **27**, 1250209 (2012).
  - [22] H. T. Feng, B. Wang, W. M. Sun, and H. S. Zong, *Eur. Phys. J. C* **73**, 2444 (2013).
  - [23] P. L. Yin, Y. M. Shi, Z. F. Cui, H. T. Feng, and H. S. Zong, *Phys. Rev. D* **90**, 036007 (2014).
  - [24] C. S. Fischer, *Phys. Rev. Lett.* **103**, 052003 (2009).
  - [25] C. S. Fischer and J. A. Mueller, *Phys. Rev. D* **80**, 074029 (2009).
  - [26] E. Bilgici, F. Bruckmann, C. Gattlinger, and C. Hagen, *Phys. Rev. D* **77**, 094007 (2008).
  - [27] G. Grignani, G. Semenoff, and P. Sodano, *Phys. Rev. D* **53**, 7157 (1996).
  - [28] J. Greensite, *Prog. Part. Nucl. Phys.* **51**, 1 (2003).
  - [29] A. Roberge and N. Weiss, *Nucl. Phys.* **B275**, 734 (1986).
  - [30] H. T. Feng, F. Y. Hou, Y. H. Xia, J. Y. Wang, and H. S. Zong, *Eur. Phys. J. C* **74**, 3216 (2014).
  - [31] H. T. Feng, X. Z. Wang, X. H. Yu, and H. S. Zong, *Phys. Rev. D* **94**, 045022 (2016).
  - [32] N. Dorey and N. E. Mavromatos, *Nucl. Phys.* **B386**, 614 (1992).
  - [33] I. J. R. Atchison, N. Dorey, M. Klein-Kreisler, and N. E. Mavromatos, *Phys. Lett. B* **294**, 91 (1992).
  - [34] P. M. Lo and E. S. Swanson, *Phys. Rev. D* **89**, 025015 (2014).
  - [35] B. Petersson, *Nucl. Phys.* **A525**, 237 (1991).
  - [36] J. B. Kogut, M. Stone, H. W. Wyld, W. R. Gibbs, J. Shigemitsu, S. H. Shenker, and D. K. Sinclair, *Phys. Rev. Lett.* **50**, 393 (1983).